

Study on Cooperative Positioning System - Optimum Moving Strategies for CPS-III -

Ryo Kurazume Shigeo Hirose

Tokyo Institute of Technology
2-12-1, Oo-okayama Meguro-ku, Tokyo 152-8552, Japan

Abstract

Several position identification methods are being used for mobile robots. Dead reckoning is a popular method but due to the accumulation error from wheel slippage, reliability is low for the measurement of long distances especially on uneven surfaces. Another popular method is the landmark method, which estimates current position relative to known landmarks, but the landmark method's limitation is that it cannot be used in an uncharted environment. Thus, this paper proposes a new method called "Cooperative Positioning System (CPS)" that is able to overcome these shortcomings. The main concept of CPS is to divide the robots into two groups, A and B respectively, group A remains stationary and acts as a landmark while group B moves and then group B stops and acts as a landmark for group A. This process is repeated until the target position is reached. Compared with dead reckoning, CPS has a far lower accumulation of positioning error, and can also work in three-dimensions. Furthermore, CPS employs inherent landmarks and therefore can be used in uncharted environments unlike the landmark method. In this paper, focus will be on the discussion of the relationship between moving configurations of CPS and its positioning accuracy for the latest prototype CPS model, CPS-III, using simulation and analytical techniques. Optimum moving strategies in order to minimize positioning error are then discussed and verified through experiments.

1 Introduction

An accurate position identification method for a mobile robot that can be used in various environments is an important consideration in the design of autonomous mobile robots. Although in recent years accurate positioning on the surface of earth has been made possible by the development of GPS, it cannot

be used underground nor inside buildings. Therefore, to realize an accurate positioning system that is able to perform based on local information about the robot and its surroundings is still an important research theme.

A number of simple techniques have been proposed based on local information such as dead reckoning, whereby mobile robots with wheels identify their current position from the number of rotations of the wheels [1],[2]. The dead reckoning method is simple and therefore easy to implement, using only internal sensors which allows the use in uncharted environments. However the dead reckoning method's drawback is that the position recorded is directly affected by the wheel contact with the ground, the type of wheel fixture, and by external disturbances such as tire slip, thus resulting in serious positioning accuracy problems over long distances and with unpaved roads or other outdoor environments. In addition, dead reckoning also cannot be used for three-dimensional positioning involving level differences.

Other, more accurate positioning techniques for mobile robots have been proposed. These techniques use optical or other sensors on the robots to detect walls, pillars, and other landmarks in the work environment [3],[4],[5]. The robots then are able to determine their positions from their positional relationship with such landmarks. The landmark method can give highly accurate positioning information over long distances and in rugged environments, but requires the previous placing of landmarks. Thus, it cannot, for example, be used for planetary exploration robots that would be in uncharted environments. With these considerations in mind, we have proposed a new method named "Cooperative Positioning System (CPS)[6]" and discussed its viability through measurement experiments using specially constructed robots [6],[7]. CPS overcomes the shortcomings of the previous two methods and thus enables position identification in

unfamiliar environments and uneven surfaces utilizing only local information stored by multiple robots.

Fig. 1 shows an example of CPS that consists of one parent robot equipped with sensors and two child robots equipped with targets for measurement.

1. While the parent robot whose initial position is measured previously remains stationary, child robots 1 and 2 travel certain distances and stops. 2. Parent robot measures distances, azimuth angles, and elevation angles from the child robot 1 with the sensors equipped, and calculates the positions of the child robot 1 3. Same thing is done for the child robot 2 5. Steps 1 to 4 are repeated until the robot group has reached the target position.

1. While the parent robot whose initial position is measured previously remains stationary, child robots 1 and 2 travel certain distances and stops.
2. Parent robot measures distances, azimuth angles, and elevation angles from the child robot 1 with the sensors equipped, and calculates the positions of the child robot 1.
3. Parent robot measures the child robot 2 in the same way as step 2
4. Parent robot travels a certain distance and stops. Then, parent robot measures distances, azimuth angles, and elevation angles from the child robots, and calculates own position.
5. Steps 1 to 4 are repeated until the robot group has reached the target position.

CPS has the following characteristics:

1. Utilizing high accuracy sensors developed for surveying to measure stationary points, CPS provides a good basis for higher positioning accuracy compared with the dead reckoning method that uses wheel rotation.
2. Unlike the landmark method, CPS does not require apriori knowledge of landmark locations. It allows measurement of position not only in foreign environments but even underground or within building where GPS cannot be used.
3. By measuring elevation angles, CPS can determine three-dimensional positions, which is not possible with dead reckoning.

From these characteristics, CPS can be used effectively as the automatic control system for robots that

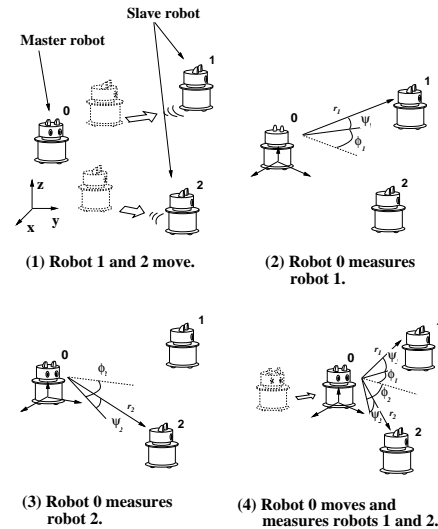


Figure 1: Example of CPS

cleans the inside of train stations or underground markets, and for exploration robots such as a planetary rover [6].

Two prototype models have been introduced named CPS-I that is equipped with laser and photo detector, and CPS-II that equipped with laser range finder and corner cubes respectively. Through measurement experiments by using these models the viability of CPS have been considered [7].

Since CPS determines position by successive measurements of relative distances and angles from stationary robots, positioning errors are accumulative and position accuracy decreases. The degree of these accumulated errors is influenced not only by the accuracy of the sensors but also by the moving strategies and movement histories of the multiple robots. With these considerations, discussions have been made of the possibility to estimate positioning accuracy of CPS for various moving strategies by assuming the measurement errors have Gaussian distributions and evaluating accumulated errors as a propagation of error variance matrixes [6].

In this paper, discussion will be made on the basic properties of accumulated errors for the latest model of CPS named CPS-III, and the optimum moving strategies to minimize the accumulated errors over long distances will be proposed. In Section 2, the basic equations will be introduced for the propagation of accumulated errors by utilizing weighted least square method. By using these equations it is possible to

realize the information fusion of various sensor data and to estimate positioning accuracy more efficiently than the previously proposed method [6]. In Section 3, the CPS third model, CPS-III will be introduced. In Section 4, moving strategies to minimize the accumulation of positioning error for CPS-III is discussed, and three moving strategies to optimize positioning accuracy are proposed. In Section 5, experimental results are shown.

2 The basic equations for the propagation of accumulated errors

This section introduces the error analytical technique utilizing weighted least square method. This method enables the information fusion of various sensor data and allows the accumulated error calculation to be treated in a systematic way.

2.1 Estimation of positioning accuracy by weighted least square method

As shown in **Fig. 1**(4), there are three robots and if the positions of two robots are already known and if the third robot is able to measure its distance, azimuth and elevation angles relative to the other two then the third robot's position can be determined as follows. We define the positions of robots 0, 1, and 2 as $\mathbf{P}_0(x_0, y_0, z_0, \theta_0)$, $\mathbf{P}_1(x_1, y_1, z_1, \theta_1)$, and $\mathbf{P}_2(x_2, y_2, z_2, \theta_2)$ and relative distances, azimuth and elevation angles from robot 0 to robots 1 and 2 as $r_1, r_2, \phi_1, \phi_2, \psi_1$, and ψ_2 . Equations that are established (observation equations) are

$$(x_0 - x_i)^2 + (y_0 - y_i)^2 = r_i^2 \cos^2 \psi_i \quad (1)$$

$$z_0 = z_i - r_i \sin \psi_i \quad (2)$$

$$\theta_0 = -\phi_i + \tan^{-1} \frac{y_i - y_0}{x_i - x_0} \quad (3)$$

for $i = 1$ and 2 . If the absolute position of robot i is $\tilde{\mathbf{P}}_i(\tilde{x}_i, \tilde{y}_i, \tilde{z}_i, \tilde{\theta}_i)$ but is measured as $\mathbf{P}_i = (\tilde{x}_i + dx_i, \tilde{y}_i + dy_i, \tilde{z}_i + dz_i, \tilde{\theta}_i + d\theta_i)$ then from the Taylor expansion of above equations

$$a_i dx + b_i dy = (r_i \cos \psi_i - d_i)$$

$$+ a_i dx_i + b_i dy_i + \cos \psi_i dr_i - r_i \sin \psi_i d\psi_i \quad (4)$$

$$dz = \tilde{z}_i - r_i \sin \psi_i - \tilde{z}_0 + dz_i - \sin \psi_i dr - r_i \cos \psi_i d\psi_i \quad (5)$$

$$-\frac{b_i}{d_i} dx + \frac{a_i}{d_i} dy - d\theta_0 = (\tilde{\phi}_i + \tilde{\theta}_0 - \tan^{-1} \frac{\tilde{y}_i - \tilde{y}_0}{\tilde{x}_i - \tilde{x}_0}) - \frac{b_i}{d_i} dx_i + \frac{a_i}{d_i} dy_i + d\phi_i \quad (6)$$

can be obtained by assuming the errors are small and the second and higher order terms may be disregarded, where $d_i = \sqrt{(\tilde{x}_i - \tilde{x}_0)^2 + (\tilde{y}_i - \tilde{y}_0)^2}$, $a_i = -\frac{\tilde{x}_i - \tilde{x}_0}{d_i}$ and $b_i = -\frac{\tilde{y}_i - \tilde{y}_0}{d_i}$.

Next, we define

$$\mathbf{A} = \begin{pmatrix} a_1 & b_1 & 0 & 0 \\ a_2 & b_2 & 0 & 0 \\ 0 & 0 & 1 & 0 \\ 0 & 0 & 1 & 0 \\ -\frac{b_1}{d_1} & \frac{a_1}{d_1} & 0 & -1 \\ -\frac{b_2}{d_2} & \frac{a_2}{d_2} & 0 & -1 \end{pmatrix} \quad (7)$$

$$\mathbf{L} = \begin{pmatrix} (r_1 \cos \phi_1 - d_1) \\ (r_2 \cos \phi_2 - d_2) \\ \tilde{z}_1 - r_1 \sin \psi_1 - \tilde{z}_0 \\ \tilde{z}_2 - r_2 \sin \psi_2 - \tilde{z}_0 \\ \phi_1 + \tilde{\theta}_0 - \tan^{-1} \frac{\tilde{y}_1 - \tilde{y}_0}{\tilde{x}_1 - \tilde{x}_0} \\ \phi_2 + \tilde{\theta}_0 - \tan^{-1} \frac{\tilde{y}_2 - \tilde{y}_0}{\tilde{x}_2 - \tilde{x}_0} \end{pmatrix} \quad (8)$$

and substitute dx_i , dy_i and dz_i as 0 by assuming previous measurements are correct, then Eqs.(4), (5), (6) are

$$\mathbf{A}\mathbf{X} = \mathbf{L} \quad (9)$$

where $\mathbf{X} = (dx_0, dy_0, dz_0, d\theta_0)^T$. Resulting in the error equation

$$\mathbf{V} = \mathbf{L} - \mathbf{A}\mathbf{X} \quad (10)$$

Furthermore the error variance of the observed value \mathbf{L} can be derived from the averages of the square of Eqs.(4), (5), and (6) as

$$\Sigma_L = \mathbf{K}_1 \Sigma \mathbf{K}_1^T + \mathbf{K}_2 \Sigma_p \mathbf{K}_2^T \quad (11)$$

where \mathbf{K}_1 and \mathbf{K}_2 are

$$\mathbf{K}_1 = \begin{pmatrix} a_1 & b_1 & 0 & 0 & 0 & 0 & 0 & 0 \\ 0 & 0 & 0 & 0 & a_2 & b_2 & 0 & 0 \\ 0 & 0 & 1 & 0 & 0 & 0 & 0 & 0 \\ 0 & 0 & 0 & 0 & 0 & 0 & 1 & 0 \\ -\frac{b_1}{d_1} & \frac{a_1}{d_1} & 0 & 0 & 0 & 0 & 0 & 0 \\ 0 & 0 & 0 & 0 & -\frac{b_2}{d_2} & \frac{a_2}{d_2} & 0 & 0 \end{pmatrix} \quad (12)$$

$$\mathbf{K}_2 = \begin{pmatrix} \cos \psi_1 & 0 & -r_1 \sin \psi_1 \\ \cos \psi_2 & 0 & -r_2 \sin \psi_2 \\ -\sin \psi_1 & 0 & -r_1 \cos \psi_1 \\ -\sin \psi_2 & 0 & -r_2 \cos \psi_2 \\ 0 & 1 & 0 \\ 0 & 1 & 0 \end{pmatrix} \quad (13)$$

And Σ is the error variance matrix for the positions of robot 1 and 2 and Σ_p is the error variance matrix for the measurement of distances, azimuth and elevation angles.

$$\Sigma = \begin{pmatrix} \Sigma_{11} & \Sigma_{12} \\ \Sigma_{21} & \Sigma_{22} \end{pmatrix} \quad (14)$$

$$\Sigma_p = \text{diag}(\sigma_r^2, \sigma_\phi^2, \sigma_\psi^2) \quad (15)$$

From Eqs.(10) and (11) the change in position of robot 0 (\mathbf{X}) that minimizes the sum of the squared remain error under the weight of Σ_L^{-1} can be derived by solving the following equation

$$\min \mathbf{V}^T \Sigma_L^{-1} \mathbf{V} \quad (16)$$

as

$$\begin{aligned} \mathbf{X} &= (\mathbf{A}^T \Sigma_L^{-1} \mathbf{A})^{-1} \mathbf{A}^T \Sigma_L^{-1} \mathbf{L} \\ &= \mathbf{B} \mathbf{L} \end{aligned} \quad (17)$$

Finally, following the next steps to calculate the optimum position of robot 0, i) assume arbitrary position of robot 0 as $\tilde{\mathbf{P}}_0$. ii) calculate $\mathbf{X} = (dx_0, dy_0, dz_0, d\theta_0)^T$ form Eq.(17). iii) repeat $\tilde{\mathbf{P}}_0 \leftarrow \tilde{\mathbf{P}}_0 + \mathbf{X}$ until $\mathbf{X} \rightarrow 0$. And thus the error variance of the position of robot 0 can be calculated form Eq.(17) as

$$\Sigma_{00} = \mathbf{B} \Sigma_L \mathbf{B}^T = (\mathbf{A}^T \Sigma_L^{-1} \mathbf{A})^{-1} \quad (18)$$

and the covariance matrixes between robots 0 and 1, and robots 0 and 2 are

$$(\Sigma_{01}, \Sigma_{02}) = \mathbf{B} \mathbf{K} \Sigma \quad (19)$$

By repeating the above steps, the positioning accuracy of the robot after performing several measurements successively can be estimated by calculating the error variance matrix and covariance matrixes from Eqs.(18) and (19).

3 CPS-III

This section introduces the latest prototype model of CPS (CPS-III shown in **Fig. 2**). CPS-III consists of one parent robot that is equipped with a high accuracy laser range finder and two child robots that are equipped corner cubes. The basic method of position identification is identical to that of the method presented in **Fig. 1**.

The master robot is equipped with a laser range finder supplied by TOPCON Ltd. (**Table 1**) that has the ability to automatically search and trace a corner cube in any arbitrary position and a 2-axis inclinometer. By detecting the laser reflected from the child robots, the master robot then automatically and accurately measures the distances and the azimuth angles from the child robots. On top of each child robot is six corner cubes arranged at intervals of 60 degrees around the vertical axis and with this mechanism a laser beam that is projected from any direction can

be accurately reflect. Each robot has a built-in microcomputer (8086-8MHz, Japan System Design Co., Ltd.), driving circuit, battery (Yuni-Z, YUASA BATTERY Co., Ltd.), and communication system (HRF-600 (RS-232C), HERUTU Co., Ltd.), and is controlled centrally from the host computer (Pentium Pro 200).

Table 1: Specifications of a range finder.

AP-L1 (TOPCON Ltd.)	
Range	4 ~ 400 [m]
Resolution (distance)	0.2 [mm]
Resolution (angle)	5 [°]
Precision (distance)	±3+2ppm [mm]
Precision (angle)	±5 [°]

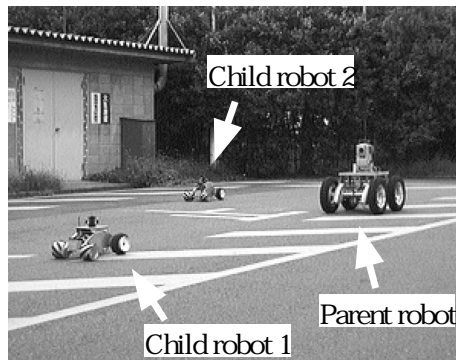


Figure 2: Total view of the mechanical model CPS-III.

4 Optimum moving configurations of CPS-III

This section discusses the relationship between the moving configuration of CPS-III and its positioning accuracy by computer simulation and analytical method, and proposes three moving strategies to optimize positioning accuracy.

First assume the following conditions.

1. CPS consists of one parent robot equipped with laser range finders and two child robots equipped with corner cubes.
2. Each robot has accurate sensors to measure its orientation around roll and pitch axis to gravity.
3. Robots move in a 2-D plane.

4. Angle and distance errors have Gaussian distributions and therefore have mean averages of zero.
5. The error variances of distance and angle measurements are constant with any measured distances and angles.

Assumption 5 is an inherent characteristic of the distance measurement sensor that utilizes a laser or electromagnetic waves. For this sensor, measurement error is not influenced by the measured distance when the distance between measurement points is close and the refractive index is not affected by temperature and humidity differences in the air. The validity of assumptions 4 and 5 have already been confirmed by iteration of error measurement experiments with CPS-III.

In addition, several other conditions need to be assumed for the computer simulations.

1. The standard deviation of the distance measurement sensors is 3 [mm] and the angle measurement sensor is 5 [sec].
2. Each robot moves along a straight line towards each target point that is placed 1 [km] ahead and the movement distance of each step is 10 [m]. Resulting in a total of 100 movements.
3. The positioning accuracy at the target position is given as a trace of parent robot error variance matrix. Error variance matrix and error covariance matrixes are calculated by Eqs.(18) and (19) at each step.
4. As shown in **Fig. 3**, robots move along the y-axis and the distances between parent and child robots are r_1, r_2 and the azimuth angles to the child robots from the parent robot are ϕ_1, ϕ_2 .

4.1 Simulation analysis

First, consider the case that the robots repeat only one type of movement by using a set of parameters r_1, r_2, ϕ_1 , and ϕ_2 to reach the target points. The moving strategy that minimizes positioning error when the robot arrives at the target position is then calculated by using Newton method. Where 32,400 initial conditions are generated by dividing the distance between robots r_1 and r_2 from 0 m to 1000 m into 10 parts, and angle ϕ_1 and ϕ_2 from 0 [deg.] to 360 [deg.] into 18 parts. From the results of these simulations, three local minimums were discovered that corresponded to the optimum moving strategies as shown in (**Table 2**).

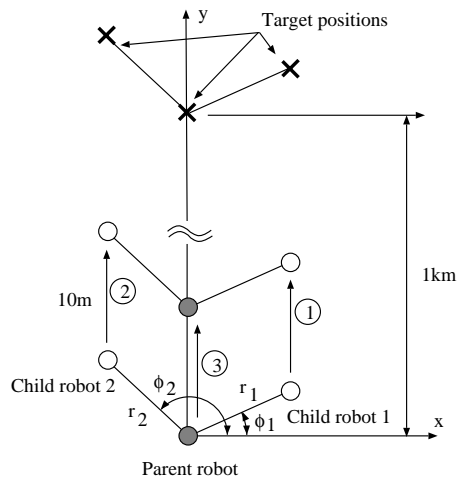


Figure 3: Simulation model.

Table 2: Optimum robots configurations.

	$r_1[m]$	$r_2[m]$	$\phi_1[deg.]$	$\phi_2[deg.]$	$\sigma_x^2 + \sigma_y^2$
A	80.3	80.3	3.0	176.1	0.0203
B	528.2	518.0	53.1	126.3	0.0218
C	72.7	106.2	89.6	-90.5	0.0207

For two local minimums A and B, both cases indicate the child robots are symmetrical towards the target direction. Local minimum for A shows all the robots are on a line perpendicular to the target direction while for B the azimuth angles to the child robots from the parent robot are $45 \sim 55[deg.]$. From here onward each is defined as optimum moving strategies A and B respectively as shown in **Fig. 4**. In addition, local minimum C is a moving strategy in which all the robots are along a line toward the target direction and from here onward is defined as optimum moving strategy C as shown in **Fig. 4**.

Next, consider the case that the robots repeat two moving strategies alternatively. In the same manner as the first case, the consecutive moving strategies that minimize positioning error at target position is calculated by using Newton method from various initial conditions. From these simulations, the moving strategies that minimize the positioning error at target positions are given as a combination of three optimum moving strategies A, B, and C found in the first case which consequently increases the likelihood that A, B, and C are part of the optimum moving strategy.

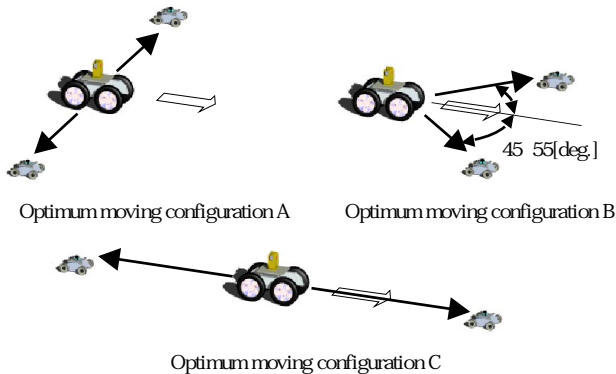


Figure 4: Optimum moving configurations.

4.2 Derivation of analytical error equation for each optimum moving strategy

As previously explained in Section 2, positioning accuracy after robot movements of a certain distance can be written as a recursive equation of the error variance matrix and error covariance matrixes from Eqs.(18) and (19). And in order to derive the answers for these recursive equations is very difficult because of the complexity of the equations. But since the robots orientation of the optimum moving strategies are symmetrical, it is possible to simplify each term of observation equations Eq.(9) so the accumulated errors of the solutions of each strategy can be easily analyzed. This section discusses these characteristics of positioning errors for the optimum moving strategies A, B, and C and considers the mechanisms that the errors occur.

4.3 Analytical solution for each optimum moving strategy

The analytical solution of positioning accuracy for optimum moving strategies A and B are shown in Appendix A. This solution shows the error variance matrix after the parent robot moves n times where the position of the parent robot is (x, y) , the positions of the child robots are $(x + d, y + h)$ and $(x - d, y + h)$, and the distance that each robot travels in y -direction is l .

Likewise, the analytical solution of positioning accuracy for optimum moving strategy C is shown in Appendix B where the child robots are along the line towards the target direction with a distance of r_1 and r_2 , and the distance that each robot travels in the y -direction is l .

From the analytical examination of these equations, the optimum conditions for each optimum moving strategy in order to minimize error variance of parent robot at target position, $\sigma_x^2 + \sigma_y^2$, is derived as shown in Table 3.

Table 3: Optimum configurations of moving strategies A, B, and C.

	$r[m]$	σ_x^2	σ_y^2	$\sigma_x^2 + \sigma_y^2$
A	70.6	0.0202	0.0003	0.0205
B	434.2	0.0201	0.0016	0.0217

	$r_1[m]$	$r_2[m]$	σ_x^2	σ_y^2	$\sigma_x^2 + \sigma_y^2$
C	63.2	90.7	0.0198	0.0009	0.0207

Also, the following characteristics are revealed from the analytical solutions of each optimum moving configuration.

1. In optimum moving configurations A and C, the measured distance and angle are used for positioning, independently. On the other hand, in optimum moving configuration B, measured distance and angle for the positioning are coupled. Thus, optimum moving configuration B is more advantageous in the case that the distance between robots is large because the angle measurement error, which increases with the distance between robots, is limited. By using analytical solutions, variation of positioning error of optimum moving strategies as a function of the distance between robots are shown in Fig. 5.
2. Optimum moving strategies are given as shown in Table 3 in any distance and angle measurement errors.

5 Experiments

Experiments to verify the validity of proposed optimum moving strategies were performed using CPS-III in a flat outdoor environment. CPS-III moved by optimum moving strategies A and C, and unoptimum moving strategy D ($\phi_1 = 80[deg.]$, $\phi_2 = 110[deg.]$) for a comparison as shown in Fig. 6. Positioning accuracy after the robots moved forward and backward 5 times was measured by the observation of fixed-points.

Experiments for each moving strategy were performed 10 times and the average positioning error

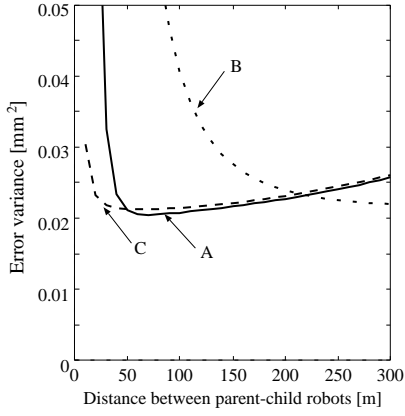


Figure 5: Variation of positioning error of optimum moving strategies A,B, and C.



Figure 6: Moving strategy D for experiments.

is compared with the corresponding analytical value (evaluated in **A** and **B**) using distance measurement error is 3 [mm] and angle measurement error is 5 [sec.] (shown in **Table 4**).

Table 4: Positioning accuracy for optimum moving strategies. Theoretical values are shown in ().

	$\sqrt{\sigma_x^2 + \sigma_y^2}$ [mm]	σ_θ [deg.]
A	100.3 (22.9)	0.387 (0.054)
C	38.2 (9.8)	0.085 (0.005)
D	175.1 (100.6)	1.162 (0.260)

Examining the results of these experiments, the positioning accuracy of optimum moving strategy C is as expected the most accurate with an error of only 28.8 [mm] (0.07% of travel distance) after 42 [m] of movement by the parent robot. In addition, the positioning accuracies of both optimum moving strategies A and C are higher than that of the unoptimum moving strategy D, which proves the effectiveness of the proposed optimum moving strategies.

6 Conclusion

This paper discusses the basic property of accumulated errors for the latest CPS model (CPS-III) using computer simulation and analytical methods. Three optimum moving strategies are then proposed for a criterion of positioning accuracy and are verified through experiments with CPS-III.

To apply CPS in actual work environments, choice of the moving strategies will become an important problem. This paper presents basic characteristics of this problem. For example, the analysis of three optimum moving strategies of CPS that may be used in different environments. Optimum moving strategy B is suitable for large open area because long distance measurement is possible without losing accuracy. On the other hand, optimum moving strategies A and C can be better adapted in environments with obstacles where the robot's field of view is hindered.

Future work will focus on CPS for specific applications, such as a planet exploration robot system or janitorial robots, and the optimizing number of robots and control methodology for positioning accuracy and adaptability in any environment.

A Analytical error solution for optimum moving strategies A and B

This section shows the derivation of the analytical error solution after each robot movement for optimum moving strategies A and B.

First, define the position of parent robot as (x, y) , the positions of child robots as $(x + d, y + h)$ and $(x - d, y + h)$, and the distance that each robot travels in the y-direction as l . Each term of the parent robot error variance matrix after the robot moves n steps can be derived by Eq.(18) as follows.

$$\Sigma_n = \begin{pmatrix} \sigma_{x,n}^2 & \rho_{xy,n} & \rho_{x\theta,n} \\ \rho_{xy,n} & \sigma_{y,n}^2 & \rho_{y\theta,n} \\ \rho_{x\theta,n} & \rho_{y\theta,n} & \sigma_{\theta,n}^2 \end{pmatrix} \quad (20)$$

If we assume the initial positioning error equals 0, then each term of the parent robot error variance matrix after 1 robot movement step is

$$\sigma_{x,1}^2 = \frac{2L_1^2 L_2^2 - d^2 l^2}{2d^2 L_2^2} \sigma_r^2 + \frac{l^2}{2} \sigma_\phi^2 \quad (21)$$

$$\sigma_{y,1}^2 = \frac{l^2 d^2 (\sigma_r^2 - L_1^2 \sigma_\phi^2) (\sigma_r^2 - L_2^2 \sigma_\phi^2) + K \sigma_r^2 \sigma_\phi^2}{2d^2 \{L_1^2 (\sigma_r^2 - L_2^2 \sigma_\phi^2) + L_2^2 (\sigma_r^2 - L_1^2 \sigma_\phi^2)\} + K \sigma_\phi^2} \quad (22)$$

$$\sigma_{\theta,1}^2 = \frac{h^2 L_2^2 + (h + l)^2 L_1^2}{2d^2 L_1^2 L_2^2} \sigma_r^2 + \sigma_\phi^2 \quad (23)$$

$$\rho_{x\theta,1} = \frac{2hL_2^2 + ld^2}{2d^2L_2^2}\sigma_r^2 - \frac{l}{2}\sigma_\phi^2 \quad (24)$$

where,

$$L_1^2 = d^2 + h^2 \quad (25)$$

$$L_2^2 = d^2 + (h+l)^2 \quad (26)$$

$$K = 2(L_1^2 + L_2^2)L_1^2L_2^2 \quad (27)$$

And each term of the parent robot error variance matrix after n robot movement steps is

$$\begin{aligned} \sigma_{x,n}^2 &= \sigma_{x,1}^2 + \sigma_{x,n-1}^2 + l^2\sigma_{\theta,n-1}^2 - 2l\rho_{x\theta,n-1} \\ &= n\sigma_{x,1}^2 + \frac{n(2n-1)(n-1)l^2}{6}\sigma_{\theta,1}^2 \\ &\quad - n(n-1)l\rho_{x\theta,1} \end{aligned} \quad (28)$$

$$\sigma_{y,n}^2 = \sigma_{y,1}^2 + \sigma_{y,n-1}^2 = n\sigma_{y,1}^2 \quad (29)$$

$$\sigma_{\theta,n}^2 = \sigma_{\theta,1}^2 + \sigma_{\theta,n-1}^2 = n\sigma_{\theta,1}^2 \quad (30)$$

$$\begin{aligned} \rho_{x\theta,n} &= \rho_{x\theta,1} + \rho_{x\theta,n-1} - l\sigma_{\theta,n-1}^2 \\ &= \rho_{x\theta,1} - \frac{n(n-1)l}{2}\sigma_{\theta,1}^2 \end{aligned} \quad (31)$$

$$\rho_{y\theta,n} = \rho_{xy,n} = 0 \quad (32)$$

B Analytical error solution for optimum moving strategy C

This section shows the derivation of the analytical error solution after each robot movement for optimum moving strategy C.

First, define the position of the parent robot as (x, y) and the child robots are along on the line towards the target direction with a distance of r_1 and r_2 , and the distance that each robot travels in the y -direction as l . Each term of the parent robot error variance matrix after n robot movement steps can be derived by Eq.(18) as follows. If we assume the initial positioning error equals 0, then each term of the parent robot error variance matrix after 1 robot movement step is

$$\sigma_{x,1}^2 = \frac{l^2(r_1^2 + r_2^2) - 2lr_1r_2(r_1 - r_2) + 4r_1^2r_2^2}{(r_1 + r_2)^2}\sigma_\phi^2 \quad (33)$$

$$\sigma_{y,1}^2 = \sigma_r^2 \quad (34)$$

$$\sigma_{\theta,1}^2 = \frac{2\{l^2 + l(r_1 - r_2) + r_1^2 + r_2^2\}}{(r_1 + r_2)^2}\sigma_\phi^2 \quad (35)$$

$$\rho_{x\theta,1} = \frac{l^2(r_1^2 - r_2^2) - 2r_1r_2(r_1 - r_2) - 4lr_1r_2}{(r_1 + r_2)^2}\sigma_\phi^2 \quad (36)$$

And each term of the parent robot error variance matrix after the n robot movement steps is

$$\begin{aligned} \sigma_{x,n}^2 &= \sigma_{x,1}^2 + \sigma_{x,n-1}^2 + l^2\sigma_{\theta,n-1}^2 - 2l\rho_{x\theta,n-1} \\ &= n\sigma_{x,1}^2 + \frac{n(2n-1)(n-1)l^2}{6}\sigma_{\theta,1}^2 \\ &\quad - n(n-1)l\rho_{x\theta,1} \end{aligned} \quad (37)$$

$$\sigma_{y,n}^2 = \sigma_{y,1}^2 + \sigma_{y,n-1}^2 = n\sigma_r^2 \quad (38)$$

$$\sigma_{\theta,n}^2 = \sigma_{\theta,1}^2 + \sigma_{\theta,n-1}^2 = n\sigma_{\theta,1}^2 \quad (39)$$

$$\begin{aligned} \rho_{x\theta,n} &= \rho_{x\theta,1} + \rho_{x\theta,n-1} - l\sigma_{\theta,n-1}^2 \\ &= n\rho_{x\theta,1} - \frac{n(n-1)l}{2}\sigma_{\theta,1}^2 \end{aligned} \quad (40)$$

$$\rho_{y\theta,n} = \rho_{xy,n} = 0 \quad (41)$$

References

- [1] Y. Fuke and E. Krotkov: Dead Reckoning for a Lunar Rover on Uneven Terrain, Proc. of IEEE Int. Conf. on Robotics and Automation, , , pp.411-416, 1996
- [2] J. Borenstein and L. Feng: Gyrodometry: A New Method for Combining Data from Gyros and Odometry in Mobile Robots, Proc. of IEEE Int. Conf. on Robotics and Automation, , , pp.423-428, 1996
- [3] K. Sugihara: Some Location Problems for robot navigation Using a Single Camera, "Computer Vision, Graphics, and Image Processing", 42, 1, pp.112-129, 1988
- [4] E. Krotkov: Mobile Robot Localization Using A Single Image, Proc. of IEEE Int. Conf. on Robotics and Automation, , , pp.978-983, 1989
- [5] M. Betke and L. Gurvits: Mobile Robot Localization Using Landmarks, IEEE Trans. Robotics and Automation, Vol.13, No.2, pp.251-263, 1997
- [6] R. Kurazume ,S. Nagata, and S. Hirose: Cooperative Positioning with Multiple Robots, Proc. IEEE Int. Conf. on Robotics and Automation, Vol. 2, pp. 1250-1257, 1994.
- [7] R. Kurazume, S. Hirose, S. Nagata, and N. Sashida: Study on Cooperative Positioning System -Basic Principle and Measurement Experiment-, Proc. IEEE Int. Conf. on Robotics and Automation, Vol. 2, pp. 1421-1426, 1996.